

3D ROBOTIC MAPPING WITH PROBABILISTIC OCCUPANCY GRIDS

Anderson A. S. Souza¹, Luiz M. G. Gonçalves²

¹Department of Informatics XYX Engineering, State University of the Rio Grande do Norte,
Natal, Brazil

andersonabner@uern.br

²Department of Computer Engineering, Federal University of the Rio Grande do Norte,
Natal, Brazil.

lmarcos@natalnet.br

ABSTRACT

We propose a new approach to 3D environment mapping from a mobile robot, using visual information provided by a low-cost stereo vision system. Depth information recovered from disparity maps serves as input for our method that uses probabilistic modelling to determine if a region is occupied or free in an occupancy grid approach. There is no similar approach in the literature, based on statistical modelling of the errors from stereo measurements and robot's motion, so this is the main contribution of this work. The resulting map can be directly used in tasks like obstacle avoidance, navigation, localization, exploration and path planning, enabling a mobile robot to perform autonomous navigation in its environment. Real experiments done with a Pioneer 3-AT mobile robot equipped with a Miniro stereowebe camera show the efficiency of our mapping approach.

KEYWORDS: Occupancy Grid, Stereo Vision, 3D Mapping.

I. INTRODUCTION

The mapping of environments is considered so far an essential task in autonomous robotics applications [1] [2]. By having knowledge about object positions and free pathways inside the environments a mobile robot can interact with them in a more flexible way. The robot can rely on the maps for safely navigating in the environments, avoiding obstacles and dealing with unexpected situations. Without a map, the detection of object positions would be more difficult and, consequently, the path planning strategy more complex.

To do this the robots need to be equipped with sensors, which enable it to collect information about its surround. Several types of sensors can be used for carrying out a mapping task. Most common are sonars, lasers and cameras. Sonars are an attractive alternative because of the associated low cost. In a previous work [3], we used a robot equipped with sonars to construct an occupancy grid map, which is based on sonars' information. It is known that this type of sensor presents significant inaccuracies in the measurements acquired. Lasers, on the other hand, are highly accurate and provide data that can produce more detailed maps [4]. However, because of its high monetary cost they are not so attractive. Cameras are sensors that are getting cheaper each day and make possible the acquisition of a large amount of data about the robot's surrounding. Besides, the advantages provided by current technological advances as light weight, small size, some embedded processing, and energy economy that make cameras a usual choice for any type of robot. The use of artificial vision systems allows the implementation of functionalities that are essential to robotics as: obstacle detection, tracking, and visual servoing. For these reasons, cameras are reaching an important role among the sensors used for robotics mapping.

Through computer vision algorithms, data coming from cameras can be mapped into a lot of improved information. From visual data, it is possible to get depth information, features as, points, lines, corners, texture, and even the geometry of objects and obstacles present in the environment. Furthermore, it is possible to estimate the motion of the robot relative to its environment, from image sequences [5].

Based on these claims, we propose a new approach for 3D robotic mapping using data provided by a stereo vision system and probabilistic methods to produce as output an occupancy grid map of the environment. By using stereo vision, a robot can collect trustable depth data anywhere, with no matter about what type of environment and characteristics present inside it. That is, there are no restrictions of the environment to be populated by specific features. In this work, we have used a low cost stereo system used to acquire visual data.

It is well known that visual data have errors which can affect the estimation process to determine the correct coordinates of the detected points with respect to a reference fixed in the world [6]. Furthermore, robot motions are inaccurate due to systematic and non-systematic factors [7]. Based on these assumptions, our mapping algorithm considers using a probabilistic approach that models the uncertainties inherent to both the sensory data and robot's motion. Thus, resulting maps are coherent with sensory information acquired by the robot. Mainly, the robot has a well-known established limit for the error, relying in more trustable information for decision making.

In this work, we performed several experiments in order to validate our approach. First, we verified the better stereo algorithm to generate a dense disparity map. Then, we confirmed the feasibility of the proposed mapping in a real environment which presents typical scenes of indoor and outdoor places.

This text is organized as follows. Following Section 2 shows the fundamentals about robotic mapping necessary to understand our approach, including the basics of the techniques for probabilistic occupancy grid construction. Section 3 presents the stereo vision problem. Section 4 introduces probabilistic modelling of the visual sensor and its uncertainties. Furthermore, this section presents the algorithm of our method. In Section 4, we validate our method with practical experiments. Section 5 makes a brief discussion about the results and points to the applications that can use the proposed technique. Section 6 gives a final analysis of our approach and ways to get it improved.

II. ROBOTIC MAPPING

Robotics mapping can be defined as the process of acquisition or construction of a spatial model of an environment using data provided by robotic sensors and devices. Several ways for representing maps are proposed in the literature. A classification largely accepted is the one proposed by Thrun [1], which classifies them in two categories: metric and topologic. A metric representation stores the geometric properties of the environment, while the topologic representation stores the connections (and their properties) between environment places.

Between the metric ones, occupancy grid model proposed by Elfes [8] is one of the most used. The occupancy grid approach is easy to construct and it can be as accurate as necessary by the task. This model represents the environment using a regular grid composed by cells, implemented by an array, in which the cells store the occupancy probability for a place of the environment. Data coming from sensors are interpreted to give an estimate of the occupancy probability of a cell. It is possible to update the cell values every time a measure is performed through a Bayesian approach.

Note that a subset of the whole representation is updated each time. This resulting probabilistic model can be used directly as a map of the environment in navigation tasks as path planning, obstacle avoidance, and pose estimation. Figure 1 illustrates the representation of a depth sensor reading in a 2D occupancy grid.

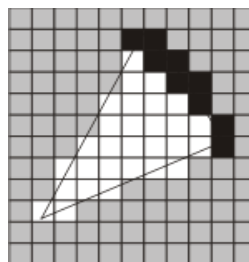


Figure 1. Occupancy grid of a range sensor reading.

Mapping using an occupancy grid representation is implemented by determining the occupancy probability of each cell. A relaxed restriction is to assume that the cells occupancy probabilities are decoupled, that is, the probability that a cell is occupied does not affect the estimation of probability occupancy values for its neighbouring cells. Besides this is not an ideal assumption specifically in the case of cells representing the same object, it makes easier to implement the mapping algorithm without a substantial increasing in the measured error. The probability of occupation of a map \mathbf{M} can be factored into the product of the occupancy probability of each cell individually, according to Equation 1.

$$P(\mathbf{M}|\mathbf{s}_{1:t}, \mathbf{z}_{1:t}) = \prod_n p(m_n|\mathbf{s}_{1:t}, \mathbf{z}_{1:t}) \quad (1)$$

The construction of the map \mathbf{M} depends of the historic of robot localizations $\mathbf{s}_{1:t}$ and of the sensors readings $\mathbf{z}_{1:t}$ performed in each localization. Updating the map is a process of repeating these readings, which can be performed from other locations with other orientations. In practice, only cells currently inside the field of view of the sensor are updated. The occupancy value of a cell m_n is calculated by Equation 2.

$$p(m_n|\mathbf{s}_{1:t}, \mathbf{z}_{1:t}) = 1 + \frac{1}{1+e^{l_{t,n}}} \quad (2)$$

Where,

$$l_{t,n} = l_{t-1,n} + \log \frac{p(m_n|\mathbf{s}_t, \mathbf{z}_t)}{1-p(m_n|\mathbf{s}_t, \mathbf{z}_t)} + \log \frac{1-p(m_n)}{p(m_n)} \quad (3)$$

The term $p(m_n)$ is the value of occupation for cell m_n previously to any measurement which can be attributed according to the obstacles density in the environment. The probability $p(m_n|\mathbf{s}_t, \mathbf{z}_t)$ specifies the occupancy probability of cell m_n conditioned to the sensor reading \mathbf{z}_t and to the robot position \mathbf{s}_t at the time t . This function is named inverse sensor model. More details of the standard algorithm for occupancy grid can be found in the work of Thrun [9].

Occupancy grids can also be used for 3D environment mapping, including information about the height of obstacles. Liu et al [10] justified the use of such approach arguing that the height information can be used to solve the data association problem in robotic mapping because 3D models have more information than 2D models, thus having less ambiguity. Moravec [11] was the first to present results of 3D occupancy grid mapping from a stereo vision system. More recent results using the same technique can be found in the work of Andert [12], however the author used a more robust model for data processing from the sensors. Different works have presented in the last years about 3D occupancy grid [13][14], however these works provide no way to deal with the uncertainties inherent to robot's motion in the map building process. This affects the credibility of the mapping.

III. STEREO VISION

The term stereo vision is generally used in the literature to nominate problems in which it is necessary to calculate real coordinates of points in a 3D scene from measurements performed from two or more images taken from different viewpoints. The determination of the 3D structure of a scene using stereo vision is a well-known problem [12]. Formally, a stereo algorithm should solve two problems: the matching (pixel correspondence) and the consequent 3D geometry reconstruction.

3.1. Stereo Matching

Matching problem can be defined as the determination of pairs of pixels, one pixel from each image in each pair, which correspond to the projection of the points detected in the scene. That is, given a pixel x in the first image, the matching problem is simply solved by determining its corresponding pixel x' in the second image. In principle, a search strategy has to be adopted to find the correspondences. Several solutions are proposed generally using restrictions to facilitate the matching. The epipolar geometry is one of these, that makes narrower the search space. This process must be executed for all pixels of the

images captured by the stereo system. Once determined the matching, disparity d can be calculated as the difference between the coordinates of the corresponding pixels in each image. Next, depth for all points in the scene can be calculated by using triangle similarity. Determination of matching for all pixels is a fundamental step. In fact, due to occlusions and image errors, we get not completely dense matching.

Between the several methods used for matching and disparity map calculation, in this work we performed experiments with the two suggested as better in the work of Scharstein and colleagues [15]: *block-matching* and *graph-cuts*. Block-matching determines the correspondence for pairs of pixels with characteristics that are well discernible. Basically, this method gives as result a disparity map in four main steps. The first is a pre-filtering of the images to normalize brightness and texture enhancement. The second step is the search for correspondences using the epipolar constraint. This step performs the summation of absolute differences between windows of the same size of both images to find the matching. As the third step, a posterior filtering is performed in order to eliminate false matching. In the fourth step, the disparity map is calculated for the trustable pixels. This method is considered fast, in fact, its computational complexity depends only on the image size.

Graph-cuts algorithm treats the best matching problem as a problem of energy minimization, including two energy terms. The smoothness energy (SE) measures the smoothness of disparity between neighbouring pixels, which should be as smooth as possible. The second term is data energy (ED) that measures how divergent are corresponding pixels with basis on assumed disparity. A weighted graph is constructed with vertices representing the image pixels. The labels (or terminals) are all the possible disparities (or all discrete values in the interval of disparity variation). The edge weights correspond to the energy terms above defined. The graph cut technique is used to approximate the optimal solution, that computes corresponding disparity values (each edge of the graph) to each pixel (vertex of the graph) [16].

3.2. Geometry Reconstruction

Geometry reconstruction is related to the determination of the scene 3D structures. The 3D position of a point P in space can be calculated by knowing the disparity between positions (in image coordinate system) of the corresponding pair of pixels x and x' , and the geometry of the system. The last is specified in two matrices M (external) and M' (internal). The positions of pixels are used in the matching to calculate the disparity map, which is then used directly in the process.

In order to better understand the stereo reconstruction problem, we consider the system shown in Figure 2. It has two cameras with optical axes perfectly parallel to each other. The baseline b (distance between each projection center) and the focal distance f are known. The two camera images are in the same plane (coplanar).

In the Figure 2, O' and O are the projection center of the cameras, f is the focal distance between the projection center and the image plane, (x'_0, y'_0) and (x_0, y_0) are the coordinates of pixels in the center of the images (intersection of optical axes and image planes). Point P in the world is projected in pixels (x', y') and (x, y) in the images. Distance z_c of the camera system to the point P can be calculated by Equation 4.

$$z_c = \frac{fb}{d} \quad (4)$$

Where b is the baseline and d is the disparity, given by $d = x' - x$. In practical situations, d is limited considering a maximum and minimum distance of the system to the scene empirically defined (calibrated). The others coordinates of the point $P_c = (x_c, y_c, z_c)$ in relation to the stereo system can be calculated by using Equations 5 and 6.

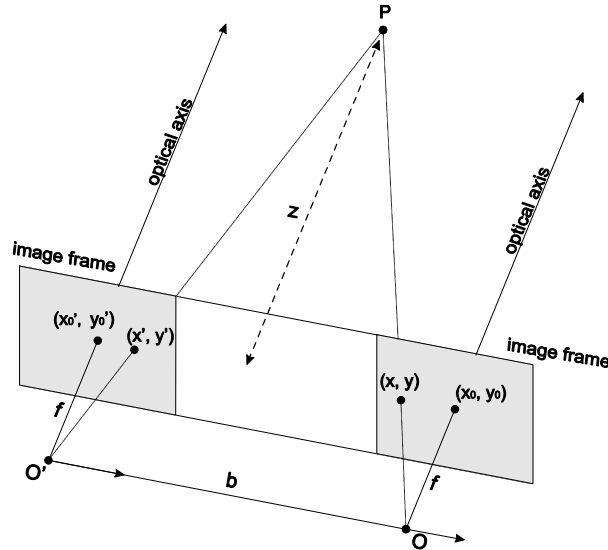


Figure 2. Stereo geometry of a coplanar camera system.

$$x_c = z_c \frac{(x-x_0)}{f} \tag{5}$$

$$y_c = z_c \frac{(y-y_0)}{f} \tag{6}$$

The coordinates of a point in the camera coordinate system P_c can be transformed to world frame. To do that, one just has to know the rotation matrix and translation vector that map the camera to world frame, and use Equation 7.

$$P_w = R^T P_c + T \tag{7}$$

Parameters $b, f, (x'_0, y'_0)$ e (x_0, y_0) are determined through a previous calibration of the stereo system. We remark that even if the system does not follow the restrictions depicted in Figure 2, it is possible to derive a general mathematical model for the problem. In this case, it would be more complex to recover the 3D geometry. Besides, in the calibration process it is also possible to diminish or eliminate errors caused by lens distortions and illumination.

IV. PROBABILISTIC MAPPING WITH STEREO VISION

In order to construct the environment representation using occupancy grid, it is necessary to model the used sensor generally named the inverse measurement model. We adopt a modelling that is similar to the one depicted by Andert [12], however we propose to incorporate both the visual data errors which affects the estimation process of the correct coordinates of the detected points in the world, and the errors inherent to robot's motion in the calculation of the occupancy probability of a cell. With this modification, we get a map that is more coherent with the sensory data provided by the robot. We can guarantee a limit for the maximum error found in the map. This is extremely important in the treatment of uncertainties encountered in the scene to the robot navigation.

The inverse sensor model transforms the data provided by the sensors in the information contained in the map. In our approach, distance measured from a specific point in the environment indicates the probability that part of the grid is occupied or free. Distance is calculated directly from disparity. In this way, it is possible to map each point of the space seen by the robot vision system with a valid disparity value into the occupancy values.

In the measurement model, each point of the disparity map can act as a distance sensor measured along the ray defined by the world coordinates of the pixel (in the image plane) and the projection center of

the camera. The point projected on the image plane is given in camera coordinates by $P_c = (x_c, y_c, z_c)$ and the distance, l_p , from the camera to P_c is calculated by Equation 8.

$$l_p = \sqrt{x_c^2 + y_c^2 + z_c^2} \quad (8)$$

Each cell m_n pertaining to this ray defined by the projection center and point P_c in world coordinates must have the occupancy probability according to the Equation 2 (section 2) which depends of the inverse measurement model given by Equation 9.

$$p(m_n | \mathbf{s}_t, \mathbf{z}_t) = p_{occ}(l) + \left(\frac{k}{\Delta l_p \sqrt{2\pi}} + 0.5 - p_{occ}(l) \right) e^{-\frac{1}{2} \left(\frac{l - l_p}{\Delta l_p} \right)^2} \quad (9)$$

Where,

$$p_{occ}(l) = \begin{cases} p_{min}, & \text{if } 0 < l \leq l_p \\ 0.5, & \text{if } l > l_p \end{cases} \quad (10)$$

This one-dimensional Gaussian model translates noisy sensory data into information of occupation, considering the uncertainties. The parameter k specifies the significance of a single measurement. The constraint $\forall l \geq l_{min}: p(m_n | \mathbf{s}_t | \mathbf{z}_t) \in [0:1]$ must be fulfilled to ensure that the resulting probabilities are valid [15]. The error, Δl_p , in the measured distance can be estimated by Equation 11.

$$\Delta l_p = \Delta z_c \frac{l_p}{z_c} + \varepsilon \quad (11)$$

In this expression we take into account the uncertainty inherent to the robot motion ε and the uncertainties in the estimation of the distance from camera to the obstacle Δz_c . The errors in the robot motion given by ε is a function modelled in our previous work [3]. The uncertainties in the distance Δz_c can be calculated by the Equation 12.

$$\Delta z_c = \frac{z_c^2}{bf} \Delta d \quad (12)$$

The acquisition and manipulation of disparity images produces an uncertainty Δd in the coordinates of the pixels, named depth resolution. Δd can easily exceed three-tenths of a pixel, which translates to a significant amount of range errors, Δz_c [6]. Figure 3 shows a typical inverse sensor model behaviour with occupancy values. Note that near distance measurements results in more significant occupancy value and far distance measurements low occupancy value.

4.1. Modelling Sensor Uncertainties

According to Xiong and colleague [6] two major error sources for a real-time stereo system in the context of the navigation of an autonomous vehicle are: foreshortening error and misalignment error. These errors can induce significant uncertainties in the estimation of the coordinate z_c , which is an important data to estimation of l_p (Equation 8). Note that l_p is important information to the inverse sensor model (Equation 11).

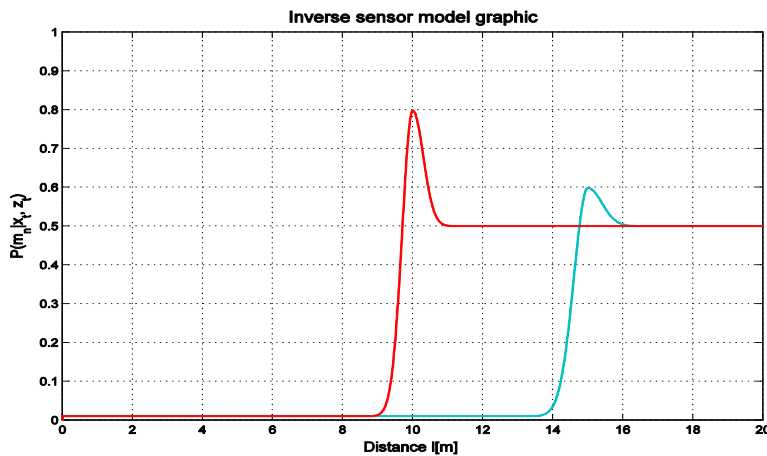


Figure 3. Inverse sensor model simulation values, with $l_p = 10m$ and $l_p = 15m$. In the red curve we have $\Delta z_c = 0.2m$ and the cyan curve $\Delta z_c = 0.3m$.

4.1.1. Foreshortening Error

Results from the fact that the 3D scene is not frontal-parallel. Therefore, for any small patch in the left image I_l , its corresponding patch in the right image I_r is not only translated but also distorted. This error, Δe_f , can be estimated by the Equation 13.

$$\Delta e_f = a \cdot e_f \tag{13}$$

where a is the disparity gradient and e_f is named foreshortening sensitivity. The gradient disparity, a , indicates if areas of the left and right images can be compared and correlated. Li and Hu [17] show a method to calculate this variable. Xiong and Matthies [6] explain how to estimate the foreshortening sensitivity, e_f .

4.1.2. Misalignment Error

The misalignment problem can be solved from a stereo calibration step. But in some terrains, like outdoor navigation there are extensive mechanical vibrations, which can often perturb camera parameters. The effects of this error can be modelled by Equation 14.

$$\Delta e_m = m \cdot e_m \tag{14}$$

Where m is the vertical misalignment and e_m misalignment sensitivity error. In some investigations [6][18], the authors suggest values in the interval [0:11; 0:31] to m , even the stereo system has been calibrated. Xiong and Matthies [6] also explain how to compute the misalignment sensitivity error e_m . The total error in the disparity estimation Δd is estimated by the sum of Equations 13 and 14, defined by Equation 15.

$$\Delta d = \Delta e_f + \Delta e_m \tag{15}$$

Δd can easily exceed three-tenths of a pixel, which translates to a significant amount of errors.

4.2. Map Build Algorithm

This subsection explains the way which the 3D map occupancy grid map is constructed from depth images. In this procedure the estimation of the occupation of each cell within the visual field of the camera is given by iterating over the pixels of the image depth, this approach is based on line drawing approach [12]. For each depth image pixel is calculated the projection ray from the camera center to the 3D coordinate of the point in the world P_w . The points on that line will have a value occupancy calculated according to the inverse sensor model (Equation 9). This procedure is represented by the Algorithm 1. Input data \mathbf{M} , D_t and \mathbf{s}_t are the grid map values estimated on time $t-1$, the depth image or disparity map and the robot position respectively. The result of this algorithm is the grid map \mathbf{M} with updated occupancy values of the cells within the visual field of the camera.

<p>Algorithm 1: BuilLocalMap</p> <p>Input: $\mathbf{M}, D_t, \mathbf{s}_t$</p> <p>Output: \mathbf{M}</p> <p>Begin</p> <p style="padding-left: 20px;">For each valid pixel from D_t do</p> <p style="padding-left: 40px;">Calculate the point P_w;</p> <p style="padding-left: 40px;">Calculate the distance l_p;</p> <p style="padding-left: 40px;">Draw a line r from camera center to P_w;</p> <p style="padding-left: 40px;">Calculate l for every cell m_n on the grid intersected by r;</p> <p style="padding-left: 40px;">Calculate the occupancy probability $p(m_n \mathbf{s}_t, \mathbf{z}_t)$ of the cell m_n;</p> <p style="padding-left: 40px;">Update the grid map \mathbf{M} by $p(m_n \mathbf{s}_{1:t}, \mathbf{z}_{1:t})$;</p> <p style="padding-left: 20px;">End</p> <p>End</p>

V. EXPERIMENTS

Initially, we have performed experiments in order to evaluate the better stereo matching algorithm to be used for the disparity map generation since we use the Minoru 3D stereo vision system and tested

firstly in indoor scenes. The implementation is done using the computer vision OpenCV library [19]. The initial results have shown that graph-cuts algorithm has achieved better results than block-matching. The disparity map generated by the graph-cuts is much richer of the weakness of the block-matching to the lack of texture in the indoor scene captured.

Next, experiments to evaluate our main proposal, the use of stereo disparity as input to the probabilistic approach in the occupancy grid construction, have been performed. We use the Pioneer 3-AT mobile robot equipped with the Minoru webcam stereo system (Figure 4), and OpenCV library for the image processing functions. The disparity map was estimated via the graph-cuts algorithm.



Figure 4: Pioneer 3-AT robot with Minoru stereo camera.

We limited the range of the visual sensor with a minimal distance $l_{min} = 0.3m$ and a maximal range $l_{max} = 3m$. The foreshortening error estimated in this experiment was $\Delta e_f = 0.04$ and the misalignment error considered is $\Delta e_m = 0.2m$. These values have resulted in a total depth resolution (or disparity error) $\Delta d = 0.24$, which can be translated in distance error as showed by Figure 5. If the distance measured from camera to an obstacle is 3m the error associated with depth resolution can produce an error in this measurement of 8cm. This uncertainties needs to be treated by the probabilistic sensor model and the correction of this errors can be achieved by updating the map.

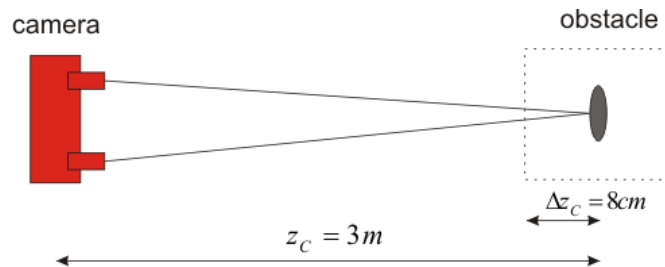


Figure 5: Sensory uncertainties given by disparity process estimation.

In order to perform the main experiment, we have chosen an environment which presents outdoor and indoor scenes, mainly a building area. Figure 6 was taken from Google Maps and shows the path executed by the robot during mapping within the environment. The dashed line represents the followed trajectory, the blue point illustrates the starting point and red point represents the end point.

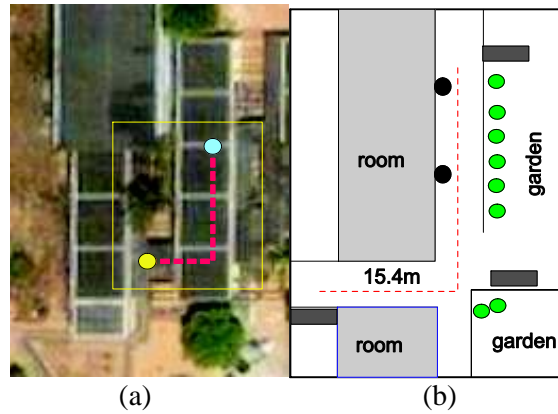


Figure 6: Path followed by the mobile robot

During the mapping the robot encountered scenes typical of indoor environments such as hallways, and outdoor scene features, such as plants. Figure 7 shows images illustrating these situations. This generality of applications is an interesting peculiarity result of joining both approaches used in this work: the occupancy grid mapping and stereo vision technique.

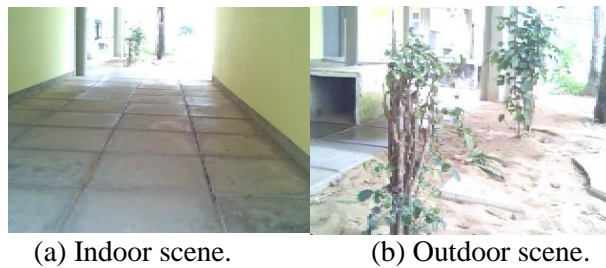


Figure 7: Distinct scenes encountered during the mapping.

In despite of these differences in scenarios, which results in different situations and difficulty in estimating the disparity map, the proposed algorithm for constructing the 3D map achieved good results as it can be seen in Figure 8. A 3D occupancy grid map is shown. In these results only the cells which the occupancy value is large enough for the robot to believe that in this place there is an obstacle, are represented. The circled area in yellow represents the 3D grid map of the scene typical of indoor and the area circled in red illustrates the map building of the outdoor scene. This result was presented with *rviz* tool, a 3D visualization environment for robots using ROS (*Robotic Operating System*) [20].

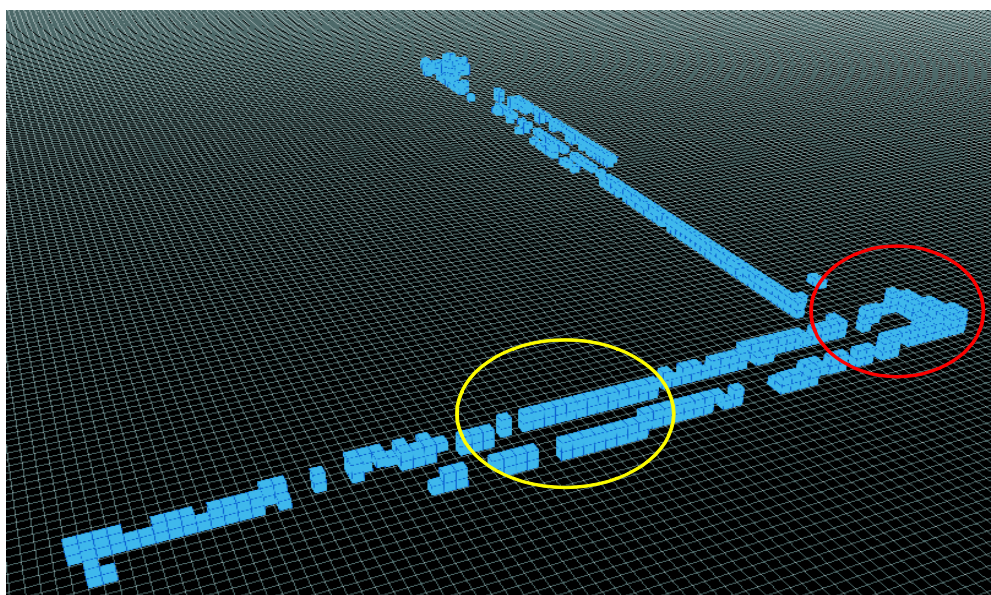


Figure 8: Resultant 3D occupancy grid.

VI. RESULTS AND DISCUSSION

The experiment shows that the proposed mapping can be used directly in tasks like path planning, obstacle avoidance, grid-based localization, etc. Furthermore, this proposed method for mapping can help a mobile robot system to reach the so desired autonomy in the execution of its tasks. Furthermore, with the resultant map the robot can identify traversable areas according to your motor skills, classifying the obstacles in the map. Higher obstacles can be assigned as non-traversable and lower obstacles can be classified as traversable point.

More complex environments require a more robust localization technique to provide the exact position of the robot. This can be achieved with *Simultaneous Localization and Mapping* technique, which allows the robot to map its environment and to calculate its position with the constructed map. Thus, tasks such as surveillance, rescue, mine exploration, firefighting, and so on, could be performed with the support of the proposed mapping.

VII. CONCLUSION

We have proposed a new approach to 3D mapping of environments by a mobile robot with map representation using a probabilistic occupancy grid. Our approach considers using the errors inherent to the robot movement in order to come up with a better modeling for the mapping algorithm. Visual information provided by a stereo vision system are included that has resulted in a more robust technique where the error can be well modeled, what is very relevant in robotics decision and applications. With our proposal, we have the mapping of environments actually coherent with sensory data provided by the robot perceptual system. This is one of the main contributions of our work, besides the manner of using stereo vision for 3D mapping using occupancy grid. As seen above, this method has been tested in applications involving indoor as well as outdoor scenes and the results show that the resulting maps are consistent with the environment.

As future work, we are already performing experimentation in more complex environments in order to test the coherent construction of 3D occupancy grids. Further, we want to implement our proposal in a SLAM (*Simultaneous Localization and Mapping*) problem, considering its application on both indoor and outdoor complex environments.

REFERENCES

- [1] Thrun, S., (2002) "Robotic mapping: A survey", *Exploring Artificial Intelligence in the New Millennium*, G. Lakemeyer and B. Nebel, Eds. Morgan Kaufmann, to appear.
- [2] Yang, S.-W. & C.-C. Wang, (2011) "Feasibility grids for localization and mapping in crowded urban scenes," in *In Proc. of IEEE International Conference on Robotic and Automation*, China, 2011, pp. 2322–2326.
- [3] Souza, A. A. S. & Santana, A. M. & Medeiros, A. A. D. & Gonçalves, L. M. G., (2010) "Probabilistic Mapping by Fusion of Range-Finders Sensors and Odometry", *Sensor Fusion and its Applications*, Sciyo.
- [4] Konrad, F. S. M. & Szczot, M. & Dietmayer, K., (2011) "Generic grid mapping for road course estimation," in *In Proc. of IEEE Intelligent Vehicles Symposium (IV)*, Baden-Baden, Germany.
- [5] Lamine, I.-K. J. T. & Berger, C. & Lacroix, S., (2007) "Vision-based slam: Stereo and monocular approaches," *International Journal of Computer Vision*, vol. 74, no. 3, pp. 343–364.
- [6] Xiong, Y. & Matthies, L. (1997) "Error analysis of a real-time stereo system," in *Proc. of IEEE Computer Society Conference on Computer Vision and Pattern Recognition*, San Juan, Jun 1997, pp. 1087–1093.
- [7] Borenstein, R. H. E. J. & Feng, L., (1996) *Where am I? Sensors and Methods for Mobile Robot Positioning*, 1st ed., Michigan, EUA.
- [8] Elfes, A., (1987) "Sonar-based real-world mapping and navigation," *Journal of Robotics and Automation*, vol. 3, no. 3, pp. 249–265.
- [9] Thrun, S., (2003) "Learning occupancy grid maps with forward sensor models," *Autonomous Robots*, vol. 15, pp. 111–127.
- [10] Liu, Y. & Emery, R. & Chakrabarti, D. & Burgard, W. & Thrun, S. (2001), "Using EM to learn 3D models with mobile robots," in *Proc. of the International Conference on Machine Learning (ICML)*.
- [11] Moravec, H. P., (1988) "Sensor fusion in certainty grids for mobile robots," *Computer*, vol. 9, no. 2, pp. 61–74, 1988.

- [12] Andert, F., (2009) “Drawing stereo disparity images into occupancy grids: Measurement model and fast implementation,” in *Proc. of IEEE/RSJ International Conference on Intelligent Robots and Systems (IROS)*, St. Louis, USA., pp. 5191–5197.
- [13] Yang, S.-W. & Wang, C.-C., (2011) “Feasibility grids for localization and mapping in crowded urban scenes,” in *Proc. of ICRA*, China, 2011, pp. 2322–2326.
- [14] Souza, A. & Maia, R. & Gonçalves, L. (2012), “3D Probabilistic Occupancy Grid to Robotic Mapping with Stereo Vision”, in *Current Advancements in Stereo Vision*, Intech, ISBN 978-953-51-0660-9.
- [15] Scharstein, D. & Szeliski, R., (2002) “A taxonomy and evaluation of dense two-frame stereo correspondence algorithms,” *International Journal of Computer Vision*, vol. 47, pp. 7–42.
- [16] Hong, L. & Chen, G., (2004) “Segment-based stereo matching using graphcuts,” in *Proc. of Conference on Computer Vision and Pattern Recognition*, pp. 74–81.
- [17] Li, Z.-N. & Hu, G., (1996) “Analysis of disparity gradient based cooperative stereo,” *IEEE Transactions on Image Processing*, vol. 5, no. 11, pp. 1493–1506.
- [18] Kim, A. I. A. W. S. & Steele, R. D., (2005) “Performance analysis and validation of a stereo vision system,” in *Proc. of IEEE System, Man and Cybernetics*.
- [19] Bradski, G. & Kaehler, A., (2008) *Learning OpenCV: Computer Vision with the OpenCV Library*, 1st ed. O’Reilly Media.
- [20] ROS.org, (2012) “Rviz documentation”, <http://ros.org/wiki/rviz>.

AUTHORS

Anderson Abner holds a Bachelor’s degree in Computer Engineering from UFRN. He has a Master’s and a Doctoral degree in Electrical and Computer Engineering with focus on robotics. Currently he teaches at The State University of Rio Grande do Norte.



Luiz M. G. Gonçalves holds a Doctorate in Systems and Computing Engineering from Federal University of Rio de Janeiro. He is an Associate Professor at the Computing Engineering and Automation Department of UFRN. He was the Chair for Brazilian Committee on Robotics and on Computer Graphics and Image Processing both under Brazilian Computer Society. His research interests are in computer vision, robotics, and graphics processing.

